

Numerical Study For The Heat Transfer By Mixed Convection Inside An Enclosure With A Top Wall Sinusoidal Motion

Lecturer. Dr. Dhia Al-Deen Hussain
Tech. Collage of Baghdad,
Dhia716@yahoo.co.uk

Asst. Prof. Dr. Nabil Jamil Yasin
Tech. Collage of Baghdad
Nabiljamil58@yahoo.com

Asst. Lect. Ayad Sleman Abdulla
Tech. Collage of Mousel
assad@yahoo.co.uk

Abstract:

Heat transfer by mixed convection of air inside an enclosure is investigated numerically. The top wall of the enclosure is assumed to oscillate horizontally with the velocity defined as $u = u_o \sin (\omega t)$. The bottom wall was subjected to a constant heat flux while the other two vertical walls were assumed to be insulated. The basis of the investigation was the two dimensional numerical solutions of the governing equations by using the finite difference method. The effects of Richardson number, Aspect ratio of the enclosure, and lid oscillation speed, on the flow and thermal behavior of the air inside the enclosure were investigated.. The results shows that the fluid flow and energy distributions within the enclosures and heat flux are all enhanced by the decrease in the Richardson number. The results are presented in the form of flow and thermal fields, and a profiles for horizontal components of velocity, temperature , and the local heat flux were also presented.

Keywords: Enclosure, Top movable wall, Mixed convection, Finite difference method.

دراسة عددية لانتقال الحرارة بالحمل المختلط داخل مغلف مع حركة موجيه للجدار العلوي

م.م. إياد سليمان داود
الكلية التقنية /الموصل

أ.م.د. نبيل جميل ياسين
الكلية التقنية / بغداد

م.د. ضياء الدين حسين علوان
الكلية التقنية / بغداد

الخلاصة

تم في هذا البحث دراسة انتقال الحرارة بالحمل المختلط داخل مغلف بافتراض ان الجدار العلوي للمغلف يتحرك حركة أفقية موجي احسب الدالة $u = u_o \sin (\omega t)$. تم تسليط فيض حراري منتظم على الجدار السفلي للمغلف بينما تم افتراض ان الجدران الجانبية معزولة عزلا تاما تم حل المعادلات الحاكمة

الثانية الإبعاد باستخدام طريقه الفروق المحددة. تم دراسة تأثير عدد ريتشاردسون، نسبة الطول الى العرض، والسرعة الموجية للجدار على التصرف الحراري للهواء داخل المغلف. أظهرت النتائج المستحصلة وجود تحسن للتوزيع الحراري للهواء مع انخفاض عدد ريتشاردسون تم ترتيب النتائج على شكل كما ان تم رسم منحنيات المركبة الفقيه للسرعة ولدرجات الحرارة ومعدل التدفق الحراري الموضوعي.

List Of Symbols

Symbols	Definition		
Y	Dimensionless length of the y-axis	AR	Height-to- length aspect ratio
ΔT_o	Temperature difference $T_h - T_c$	Gr	Grashof number
Nu_{ave}	Average Nusselt number	Re	Reynolds number
S	Dimensionless frequency	Ri	Richardson number
H	Height of the enclosure(m)	U	Dimensionless horizontal velocity
L	Length of the enclosure(m)	V	Dimensionless vertical velocity
u	Horizontal velocity component	Pa	Dimensionless period
v	Vertical velocity component	Pr	Prandtl number
u_o	Amplitude of the oscillation	Nu	Nusselt number
g	Acceleration due to	Δp	Differential pressure
gravity(m/s ²)		x	Dimensional length of the x-distance
P	Pressure(N/m ²)	X	Dimensionless length of the x-axis
		y	Dimensional length of the y-distance
		T	Time(sec)

Greek symbols

ψ	Stream function	W	Vorticity
α	Thermal diffusivity	Ψ	Dimensionless stream function
ω	Angular frequency	Ω	Dimensionless vorticity
μ	Viscosity (m ² /s)	τ	Dimensionless time
ν	Kinematic viscosity (m ² /s)	θ	Dimensionless temperature
ρ	Density (Kg/m ³)	β	Thermal expansion coefficient

Subscripts

Symbols	Definition
C	Cold
H	Hot

1. Introduction

The problem of heat transfer by mixed convection has been the subject of intensive theoretical, numerical, and experimental investigations in the recent years because of its significant applications in nature and in many scientific and engineering practices. The analysis of mixed convective flow in the enclosures and cavities is found in many applications, such as in heat exchangers, ventilation of rooms, solar energy collection, chemical processing equipment, microelectronic cooling, crystal growth in liquids, and have attracted many researchers [1,2]. The analysis of heat transfer by mixed convection in the enclosures is very complex due to the interaction of the shear driven force and the buoyancy effects. The flow governing dimensionless parameter, Richardson number, (Ri), is defined as the ratio of the Grashof number, (Gr), to the square of the Reynolds number, (Re). The Richardson number is a measure of the relative importance of the buoyancy- driven natural convection to the lid-driven forced convection. Depending on the values of the Richardson number, the problem of the combined shear and buoyancy-driven convection can be classified into three flow regimes as follows; pure forced convection for $Ri \ll 1$, mixed convection for $0.1 \leq Ri \leq 10$, and pure natural convection for $Ri \gg 1$, O [3,4,5].

Many researchers have studied the mixed convection heat transfer problems. These studies are conducted to investigate the effects of Richardson number, aspect ratio and the Prandtl number on the characteristics of the flow and thermal fields. Iwatsu et al. [6] investigated the effect of an external excitation on the flow characteristics of a viscous fluid in a square cavity numerically. In their model, the top sliding wall with sinusoidal oscillations drove the flows. They found that an enhancement in heat transfer rate was obtained at particular lid frequencies. Aydin and Yang [7] investigated the heat transfer mechanism on a laminar mixed convection in a shear- and buoyancy-driven cavity with the fraction of its lower wall heated and cooled from moving upper wall. They found that for the ratio of the length of the heated portion of the lower wall to the entire length of the enclosure, equals to 0.2. The mixed convection region with comparable shear and buoyancy forces is more effective for the range $0.5 \leq Ri \leq 2$, which increases with the ratio. Mixed convection heat transfer in a two-dimensional rectangular cavity with constant heat flux from partially heated bottom wall with isothermal sidewalls moving in the vertical direction, was studied by Guanghong et al. [4]. Their results indicate improve flow and temperature fields With the increase the Richardson number and dimensionless length of the heat source.

Khanafer et al. [8] investigated the effects of oscillatory motion of the upper wall. Their obtained results reveal that the Reynolds and Grashof numbers would either enhance or retard the energy transport process and drag force behavior depending on the velocity cycle. Mahmud [8] investigated mixed convection fluid flow and heat transfer in lid-driven rectangular enclosures filled with the Al_2O_3 -water nanofluid The object from his work was study the effects of the Richardson number, the aspect ratio of the enclosure and the volume fraction of the nanoparticles on the fluid flow and heat transfer inside the enclosure. The results shows that for the range of the Richardson number considered, 10^{-1} to 10^1 , the average Nusselt number of the hot wall, increases with increasing the volume fraction of the nanoparticles.

2. Problem Analysis

Periodic mixed convection in the square enclosure filled with air was considered for the present study with the physical dimensions as shown in the **Figure .(1)**. The Bottom wall of the enclosure is maintained at higher temperature than its top wall while the vertical walls are assumed to be perfectly insulated. The top wall oscillates compulsorily and horizontally with variable velocity according to $u=u_0\sin(\omega t)$, in which (t) is time, (u_0) is the amplitude of the oscillation, and (ω) is the angular frequency of the motion.

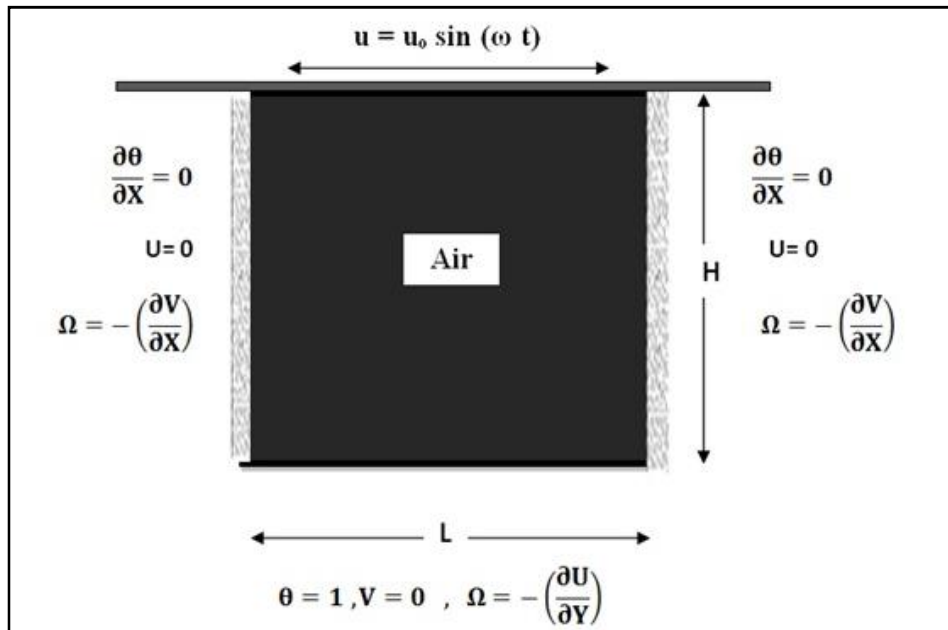


Fig .(1) schematic representation of the physical model

The flow of the enclosed fluid is considered to be two-dimensional, incompressible, and laminar. The fluid is assumed to be Newtonian and all other properties of the fluid were considered to be constant, the density is treated as constant in the continuity equation and the inertia term of the momentum equation but allow changing with temperature in the gravity term of the momentum equation, this assumption known as Boussinesq approximation. The heat transfer by radiation is neglected.

The governing equations for the system of the enclosed fluid are the expression for the conservation of mass, momentum, and energy transports at every point of the system within the limit of the basic assumptions and the use of appropriate boundary conditions. These equations which can be seen in any classical textbook of heat transfer ^[10] are stated for a two-dimensional rectangular domain in Cartesian coordinates as follows:

The continuity equation for unsteady state two dimensions flow condition, in the x- and y directions respectively:

$$\frac{\partial u}{\partial x} + \frac{\partial v}{\partial y} = 0 \text{ ----- (1)}$$

The momentum equations, for unsteady state two dimensions flow condition, in the x- and y directions respectively:

$$\frac{\partial \mathbf{u}}{\partial t} + \mathbf{u} \frac{\partial \mathbf{u}}{\partial x} + \mathbf{v} \frac{\partial \mathbf{u}}{\partial y} = -\frac{1}{\rho} \frac{\partial p}{\partial x} + \nu \left(\frac{\partial^2 \mathbf{u}}{\partial x^2} + \frac{\partial^2 \mathbf{u}}{\partial y^2} \right) \quad \text{--- --- --- (2)}$$

$$\frac{\partial \mathbf{v}}{\partial t} + \mathbf{u} \frac{\partial \mathbf{v}}{\partial x} + \mathbf{v} \frac{\partial \mathbf{v}}{\partial y} = -\frac{1}{\rho} \frac{\partial p}{\partial y} + \nu \left(\frac{\partial^2 \mathbf{v}}{\partial x^2} + \frac{\partial^2 \mathbf{v}}{\partial y^2} \right) + \beta g(T - T_c) \quad \text{--- --- --- (3)}$$

Where $\beta g(T - T_c)$ stands for the buoyancy force term which is the body force per unit volume in the Y-direction. The Boussinesq approximation for density variation with temperature is expressed as

$$\rho = \rho_c(1 - \beta(T - T_c)) \quad \text{--- --- --- (4)}$$

The thermal energy transport equation is:

$$\rho c_p \left(\frac{\partial T}{\partial t} + \mathbf{u} \frac{\partial T}{\partial x} + \mathbf{v} \frac{\partial T}{\partial y} \right) = k \left(\frac{\partial^2 T}{\partial x^2} + \frac{\partial^2 T}{\partial y^2} \right) \quad \text{--- --- --- (5)}$$

The Navier–Stokes equations (2) and (3) are reduced into one non-dimensional equation by the introduction of the expressions describing the velocity components as the derivatives of the stream function

$$\mathbf{u} = \frac{\partial \psi}{\partial y} \quad \mathbf{v} = -\frac{\partial \psi}{\partial x} \quad \text{--- --- --- (6)}$$

the vorticity equation,

$$\mathbf{W} = \frac{\partial \mathbf{v}}{\partial x} - \frac{\partial \mathbf{u}}{\partial y} \quad \text{--- --- --- (7)}$$

and the dimensionless parameters

$$\mathbf{U} = \frac{\mathbf{u}}{u_o}, \mathbf{V} = \frac{\mathbf{v}}{u_o}, \theta = \frac{T - T_c}{T_h - T_c}, \tau = \frac{t \cdot u_o}{H},$$

$$p = \frac{\bar{P}}{\rho u^2} \quad \text{where} \quad \bar{P} = P + \rho g h$$

$$\mathbf{P}_m = \mathbf{P} - \mathbf{P}_o, \quad X = \frac{x}{H}, \quad Y = \frac{y}{H},$$

$$\Omega = \frac{W}{u_o}, \quad \Psi = \frac{\psi}{u_o H}, \quad S = \omega H / u_o$$

$$Pd = 2\pi/S$$

The results of the analysis are the stream function equation describing the flow kinematics:

$$\frac{\partial^2\Psi}{\partial X^2} + \frac{\partial^2\Psi}{\partial Y^2} = -\Omega \quad \text{-----} \quad (8)$$

and the vorticity transport equation

$$\frac{\partial\Omega}{\partial\tau} + U\frac{\partial\Omega}{\partial X} + V\frac{\partial\Omega}{\partial Y} = \frac{1}{Re}\left(\frac{\partial^2\Omega}{\partial X^2} + \frac{\partial^2\Omega}{\partial Y^2}\right) + Ri\frac{\partial\theta}{\partial X} \quad \text{-----} \quad (9)$$

The energy equation (5) is also non-dimensionalized to give

$$\frac{\partial\theta}{\partial\tau} + U\frac{\partial\theta}{\partial X} + V\frac{\partial\theta}{\partial Y} = \frac{1}{Re\ Pr}\left(\frac{\partial^2\theta}{\partial X^2} + \frac{\partial^2\theta}{\partial Y^2}\right) \quad \text{-----} \quad (10)$$

The principal non-dimensional parameters appearing in the above equations are the Reynolds number, (Re), the Prandtl number, (Pr), and the Richardson number, (Ri).

In this work, the problem governing equations (8) – (10) are solved numerically with the prescribed boundary conditions for the velocity, stream function, vorticity, and temperature fields in dimensionless form

- 1- The bottom of enclosure, $Y = 0, 0 \leq X \leq AR$

$$\theta = 1, V = 0, \Omega = -\left(\frac{\partial U}{\partial Y}\right) \quad \text{-----} \quad (11)$$

- 2- The Top of enclosure at, $Y = 1, 0 \leq X \leq AR$

$$\theta = 0, V = 0, U = \sin S\tau, \Omega = -\left(\frac{\partial U}{\partial Y}\right) \quad \text{-----} \quad (12)$$

- 3- The left side (insulated boundaries), $X=0, 0 \leq Y \leq 1$

$$\frac{\partial\theta}{\partial X} = 0, U = 0, \Omega = -\left(\frac{\partial V}{\partial X}\right) \quad \text{-----} \quad (13)$$

- 4- The right side (insulated boundaries), $X=AR, 0 \leq Y \leq 1$

$$\frac{\partial\theta}{\partial X} = 0, U = 0, \Omega = -\left(\frac{\partial V}{\partial X}\right) \quad \text{-----} \quad (14)$$

The vorticity is obtained by a Taylor series out from the wall and is independent of the wall orientation.

The local heat transfer coefficient $h=q''/[T_h - T_c]$ at a given point on the heat source surface where T_h is the local temperature on the surface. Accordingly the average Nusselt number

$$\overline{Nu} = \frac{hH}{K} = \frac{[q''/(T_h - T_c)]H}{K} \quad \text{-----} \quad (15)$$

$$q'' = -k \frac{\partial T}{\partial y} \quad \text{-----} \quad (16)$$

Where

$$\partial Y = \frac{1}{H} (\partial y) , \quad \partial \theta = \frac{1}{T_h - T_c} (\partial T)$$

$$Nu = -H \frac{1}{T_h - T_c} \frac{\partial T}{\partial y} = -H \frac{\partial \theta}{\partial y} = - \frac{\partial \theta}{\partial Y} \quad \text{-----} \quad (17)$$

the average Nusselt number

$$Nu_{ave} = \frac{1}{AR} \int_0^{AR} \left(- \frac{\partial \theta}{\partial Y} \right) dX \quad \text{-----} \quad (18)$$

3. Numerical Solution

The governing equations (8) – (10) together with the boundary conditions were solved numerically using finite difference method, which reduces the continuum problem to a discrete problem prescribed by a system of algebraic equations. The vorticity transport and energy equations were solved using the Alternating Direction Implicit (ADI) method and the stream function equation was solved by the Successive Over Relaxation (SOR) method. The first and second spatial derivatives of the equations were thereby approximated by the central difference scheme, while the second order upwind difference scheme was used to discretize the convective non-linear terms due to its better stability and convergence of the computation process since the direction of the flow was considered. The resulting systems of linear algebraic equations were solved iterative using successive relaxation method.

At time $t = 0$, the values for the temperature, the stream function, the vorticity, and the velocity components at all the interior grid points were set to zero. The solution algorithm was such that the temperature distribution was foremost determined by solving the energy transport equation. This was followed by the computation of the vorticity and the stream function fields. The wall vorticities were updated from the solution of the stream function equation, while the velocity components were obtained in the dimensionless form from equation(6). The steady state was determined by monitoring the convergence of the temperature, stream function, and the vortex fields using the relative error test

$$\sum_{i=2, j=2}^{i=N_i-1, j=N_j-1} |\Phi_{(i,j)}^{k+1} - \Phi_{(i,j)}^k| < E_{max} \quad \text{-----} \quad (19)$$

The parameter Φ stands for θ, Ψ, Ω , and k denotes the number of iterations. The value of E_{\max} used as stated in different literatures varies between 10^{-3} and 10^{-8} . A value of equals 10^{-4} was however used in this work because any further reduction in this value did not yield any change in the result of the computed fields.

4. Results And Discussion

At the first step the present computer code was validated by comparing the results with other researches. The accuracy and the reliability of the code used in this work were tested by checking the grid refinement sensitivity of the results generated on the average Nusselt number for Richardson number in a square enclosure. The optimal number of nodes were determined when the solution was in terms of main quantity of interest, such as average Nusselt number, It was nearly independent of the number of nodes considered. **Figure.(2)** shows the effect of grid fineness on the average Nusselt number on the hot surface. The number of iteration step required to satisfy the convergence condition, is increasing with decreasing the grid size, in other word, increasing the number of grids.

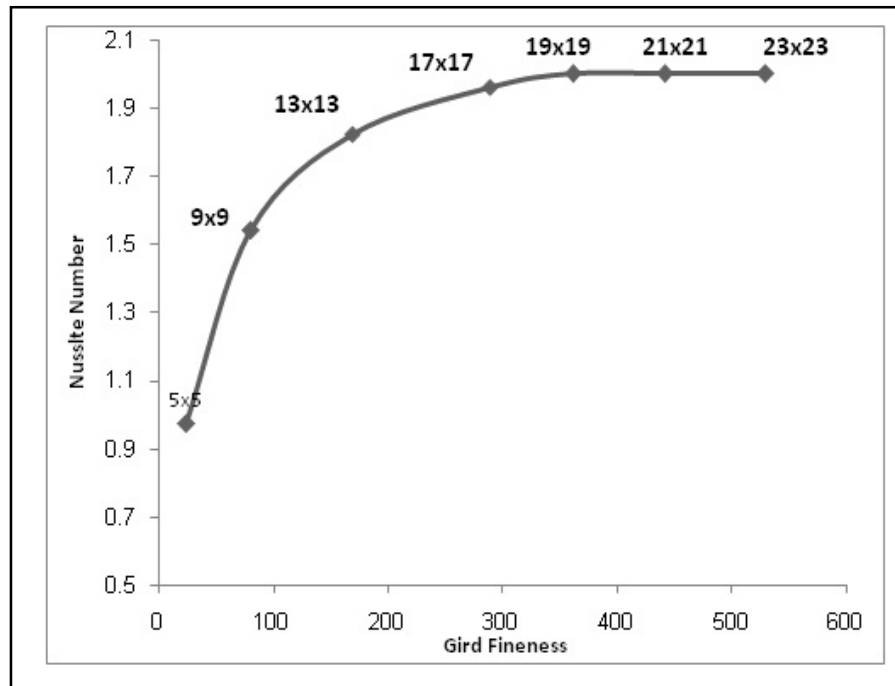


Fig .(2) the Nusselt number according to grid size, Ri=0.01

This practice is always a balance of convergence and computational time. Equal spacing grid of (21x21) can be expected to yield acceptable accuracy. It is important to validate the present calculation by trying to duplicate the results obtained by different investigators. **Table (1)** shows excellent agreement between the present numerical results in terms of the average

Nusselt number along the hot wall, under the effect of Richardson number equal (0.01), and other numerical results which obtained from previous works.

The steady state results obtained from the solution of transient equations (8)–(10) subject to the boundary conditions (11) and (14) presented in terms of the streamline and isotherm patterns, and the profiles of the velocity, temperature and the local Nusselt number.

Table (1): Comparison of the average Nusselt number computed in this work with those of the previous works at Richardson number, $Ri = 0.01$.

Ri	Present results	Khanafer et al. ^[8]	Iwatsu et al. ^[6]	Abdelkhal ek ^[9]
0.01	2.0	2.02	1.940	1.9850

4.1. The effect of the upper plate speed on the dimensionless parameters, velocity and temperature

Figures 3, 4 and 5 shows the streamlines and isotherms inside the enclosure with aspect ratio ($AR=1$) for various Richardson numbers ($Ri=1, 0.01, \& 100$) at different period times for dimensionless plate oscillation frequency ($S=2$). The flow is established by moving the top plate to produce $Ri=1$, the thermal and flow field shows an interaction between forced and natural convection flow as in **Figure.(3)**. The flow field is presented in the form of lines at constant stream function consist of one cell pattern, affected mainly by the oscillating speed of the top wall. For $Ri=0.01$, it can be observed from **Figure .(4)** that the forced convection is the dominant regime while the effect of natural convection seems to be less ,that is mainly due to the increasing of the amplitude of the top wall oscillation speed. Also the figure shows that the flow field consists of one cell at different period's time. With increasing of Richardson number ($Ri=100$) **Figure .(5)**, the fluid flow inside the enclosure dominated by natural convection. This can be clearly seen from the distribution of the isotherm in the figure. The flow field will shows to be consist from two cells occupies all the space inside the enclosure. **Figures (6) and (7)** shows the variation of horizontal component of dimensionless parameters (U) and (Θ) respectively across the vertical mid-plane of the enclosure ($X=0.5$) for Richardson number ($Ri=0.01$) with aspect ratio ($AR=1$) and ($S=2$) at different period times. From **Figure.(6)** we can observe that the velocity component is increasing with y -coordinates towards the top wall. This is attributed mainly to the shear stress which developed by the oscillating moving of the applied at the bottom wall. It has been observed that there is a coinciding between the profile of the thermal and flow fields for the periods of ($0 Pd \& 1 Pd$), as well there is a mirror symmetry in the ($1/4 Pd \& 3/4 Pd$) & ($0 Pd$ with $1/2 Pd$) due to the sin-motion of the upper plate.

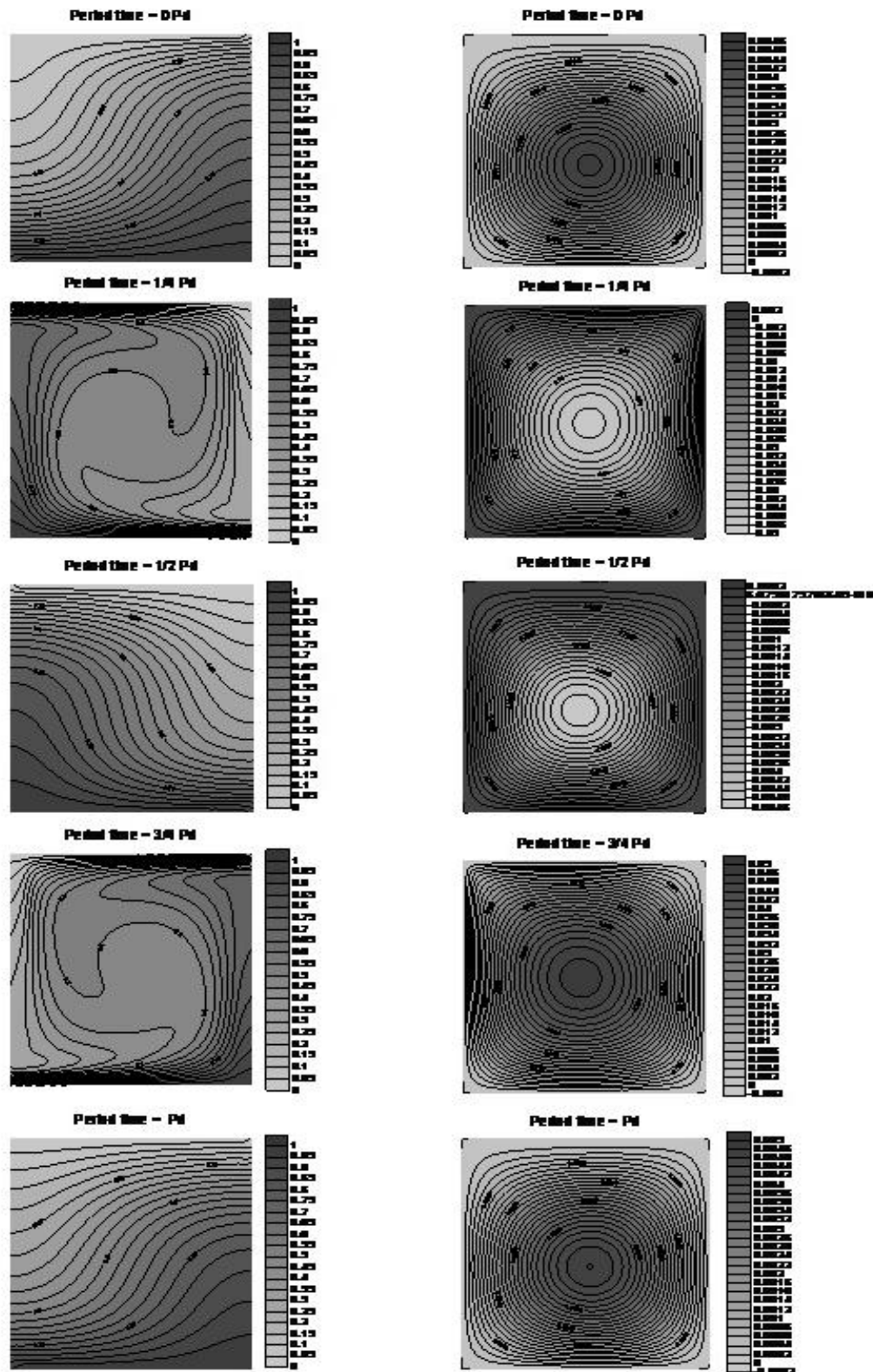


Fig.(4).Thermal field (left)and flow field (right) for $Ri=0.01$, $S=2$, $AR=1$

Fig .(4) Thermal field (left) and flow field (right) for $Ri=0.01$, $S=2$, $AR=1$

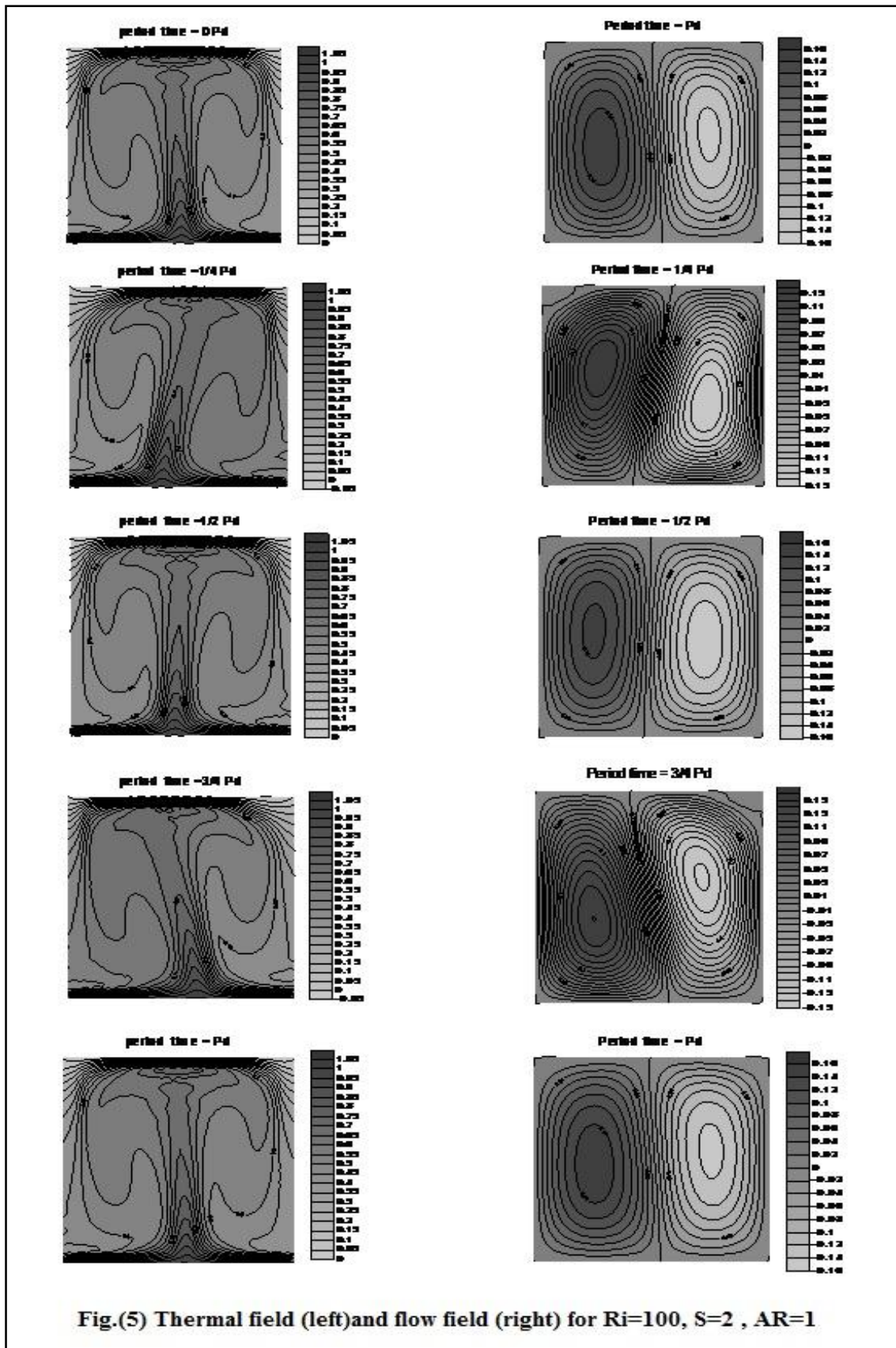


Fig.(5) Thermal field (left)and flow field (right) for $Ri=100$, $S=2$, $AR=1$
 Fig .(5) Thermal field (left) and flow field (right) for $Ri=100$, $S=2$, $AR=1$

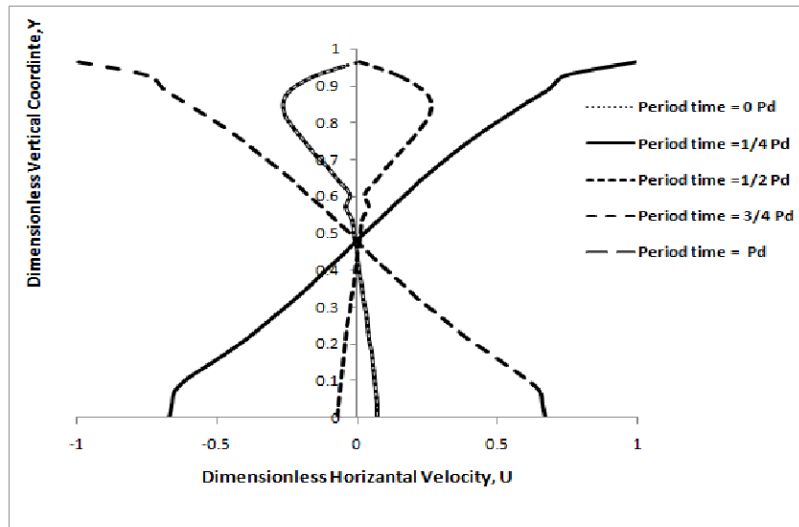


Fig .(6) variation of U along the vertical centerline Ri= 0.01 at different period time

Figure. (7) represent the variation of the temperature profiles for different (Pd), for (Ri=0.01) which showing that the gradient of temperature curves in the enclosure decreases with y-coordinate towards the top wall as a result of the forced motion of the wall which dominate the buoyancy effect in the core of the enclosure..

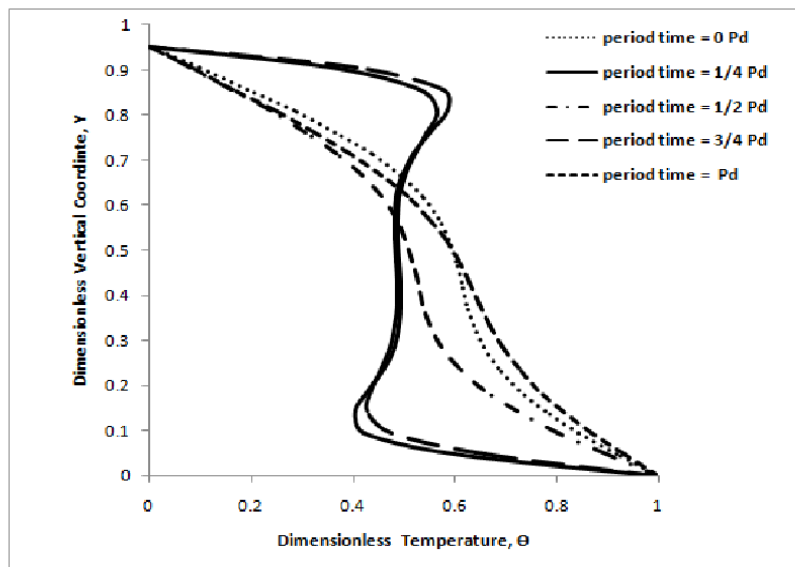


Fig. (7) Variation of θ along the vertical centerline for $Ri = 0.01$ at different Period time

Figure .(8) shows the variation of horizontal component of dimensionless velocity (U), along

The vertical centerlines at ($Ri=1$) for the same time periods as in Fig.(6). It is clear

from **Figure .(8)** that the flow speed near the top wall is less than that when ($Ri=0.01$)

shows in **Figure .(6)** and the flow velocity at the bottom wall is greater than that of ($Ri=0.01$),

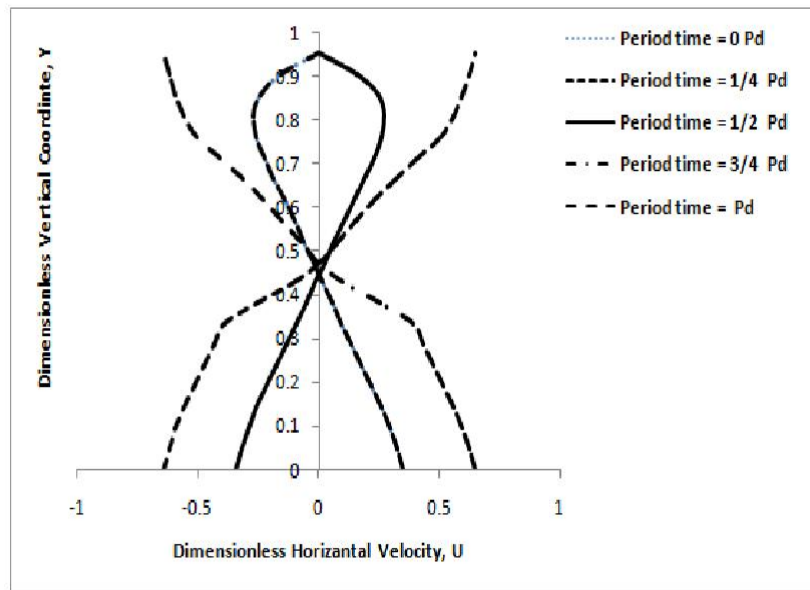


Fig. (8) Variation of U along the vertical centerline for $Ri = 1$ at different Period time

that was due to the effect of the force convection at the top wall which seems to be less comparing with that when ($Ri=1$). The flow velocity at the top and bottom wall are shown to be equal because the equality of the shear stress developed by the moving of the upper plate with the buoyancy forces induced by the heat applies at the bottom wall.

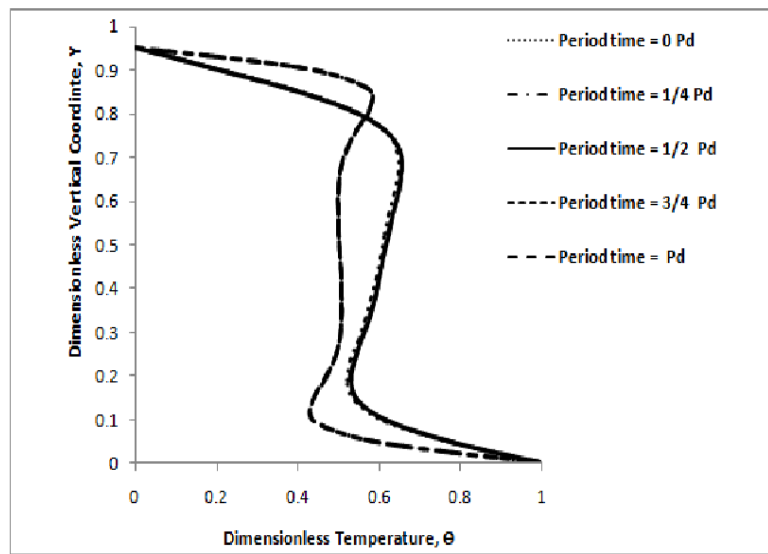


Fig. (9) Variation of θ along the vertical centerline for $Ri = 1$ at different Period time

Figure.(10) shows the variation of (U) along the vertical centerlines at ($Ri=100$) for the same time period as in Figures.(6) and (8). From this figure we can observe that the fluid flow velocity gradient is decrease with y -coordinate towards the top wall. Comparing with the previous

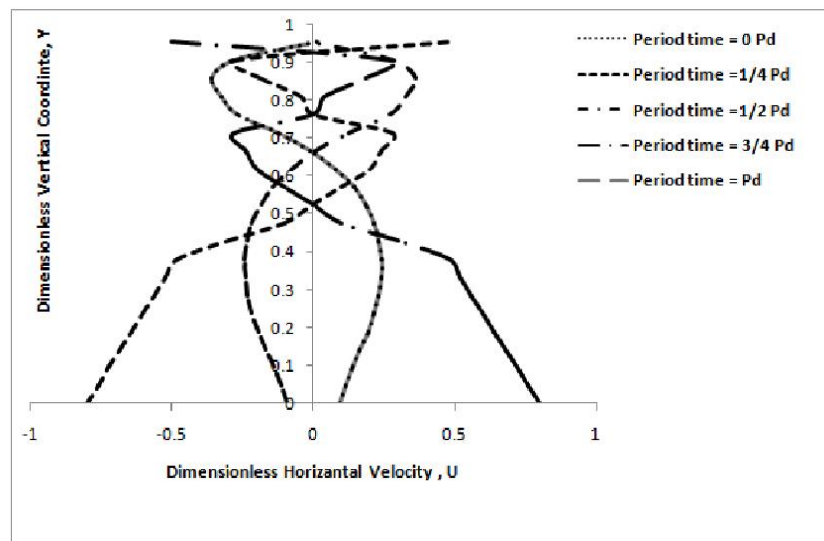


Fig. (10) Variation of U along the vertical centerline for $Ri = 100$ at different Period time

cases, the flow velocity at the bottom wall is more than that when ($Ri=1$) as in Figure.(8) and ($Ri=0.01$) as in Figure.(6) for the same time period, that is because the buoyancy motions dominate the forced motion in the core of the enclosure.

Figure.(11) shows that the temperature values (Θ) at the top wall when ($Ri=100$) is greater than that when ($Ri=0.01$) and ($Ri=1$) shown in **Figure.(7)** and in **Figure.(9)** respectively, for the same time periods. The reduction in the velocity amplitude of the top wall causes a reduction in force convection heat transfer, combine with Ri increase. This will cause heat accumulation at the top wall, which is produce high temperature with increasing Richardson number.

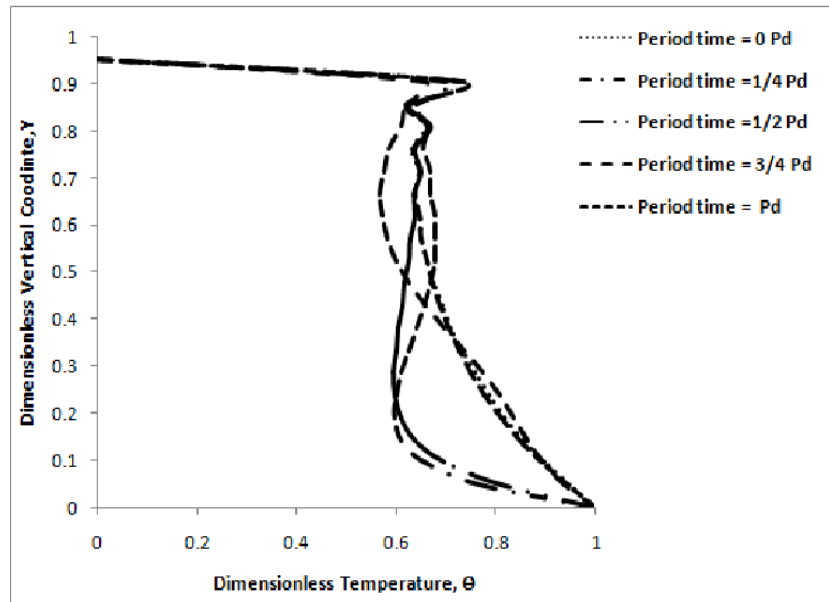


Fig. (11) Variation of θ along the vertical centerline for $Ri = 100$ at different Period time

Comparing **Figure.(7)** with **Figures (9 & 11)** for ($Ri=1$ & 100) respectively, we can observe that the temperature gradient decreases with the increases of Richardson number due to the evolution of flow stratification. **Figure.(12)** presents the variation of average Nusselt number versus time for $Ri=0.01, 1, 100$ and $S=2$ with aspect ratio $AR=1$. For all values of Richardson numbers, Nusselt number, starts to increase from zero with some delay. The delay time is more noticeable at low Richardson numbers. After the first cycle the periodic Nusselt number reached its maximum value. This maximum value of periodic Nusselt number starts to decrease from its initial high value until it reaches a periodic steady state condition value. The periodic steady state condition is reached faster at high Richardson numbers. Also from **Figure.(12)** it is shown that maximum value of Nusselt number increased when the Richardson number is decreased. This is because the amplitude of wall oscillations is high at low Richardson number, $Ri=0.01$. Therefore, forced convection is a dominant regime and a better heat transfer is achieved.

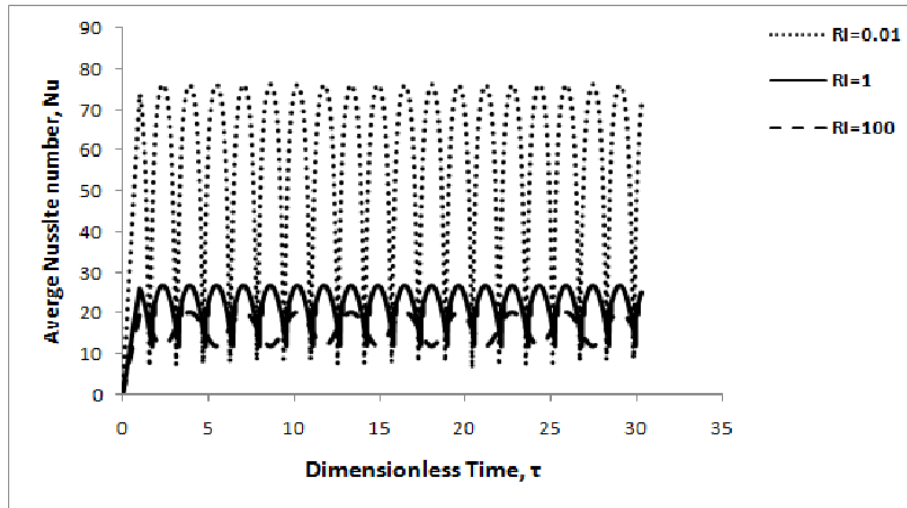


Fig. (12) The effects of the Richardson number, Ri , on the Average Nusselt number at $S=2$ and $AR=1$

4.2. Effect of Aspect Ratio (AR)

The profiles of average Nusselt number are presented in **Figure.(13)** to illustrate the influence of the aspect ratio on the heat flux to the enclosure at ($Ri=1$).

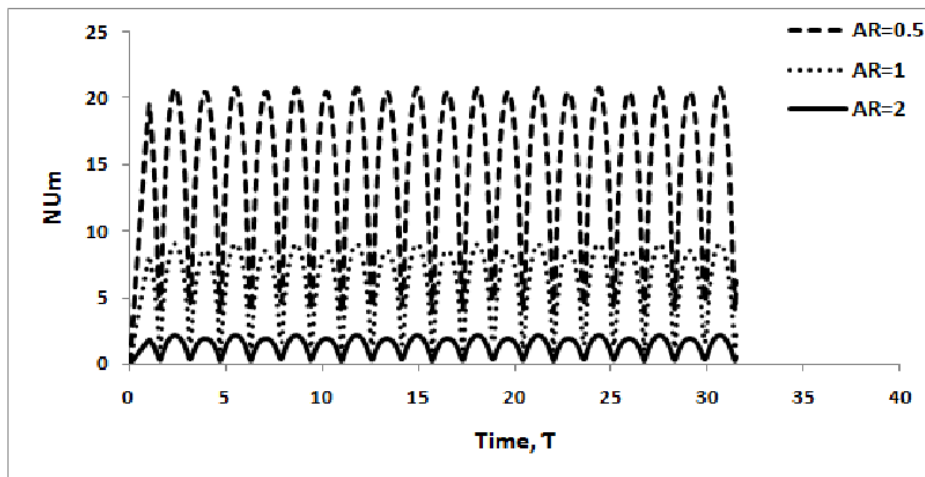


Fig. (13) The effects of the Aspect Ratio , AR , on the Average Nusselt number at $Ri=1$

The Figure show that higher heat flux is predicted for an aspect ratio of (0.5). The profiles of the curves for the aspect ratios of (1 and 2) are almost similar expect as they have two points of inflection due to the flow fields that are characterized by two symmetric cells.

4.3. Effect of oscillation frequency

The effect of oscillation frequency (S) of the top wall on the periodic steady state average heat transfer rate (in terms of average Nusselt number, Nu_{ave}) has been studied while Richardson number is assumed constant ($Ri=1, 100$). The variations of Nu_{ave} along the cold and hot walls with (S) are presented in **Figure.(13)** & **Figure.(14)** respectively. The results show that as the oscillation frequency of the sliding top wall (S) decreases, the oscillation amplitude of the average Nusselt number increases. The main reason for this behavior is that as the wall oscillates with a higher frequency, there is not enough time for the interaction between the shear and buoyancy effects, whereas at lower frequencies, the shear forces can either strengthen or weaken the buoyant fluid flow.

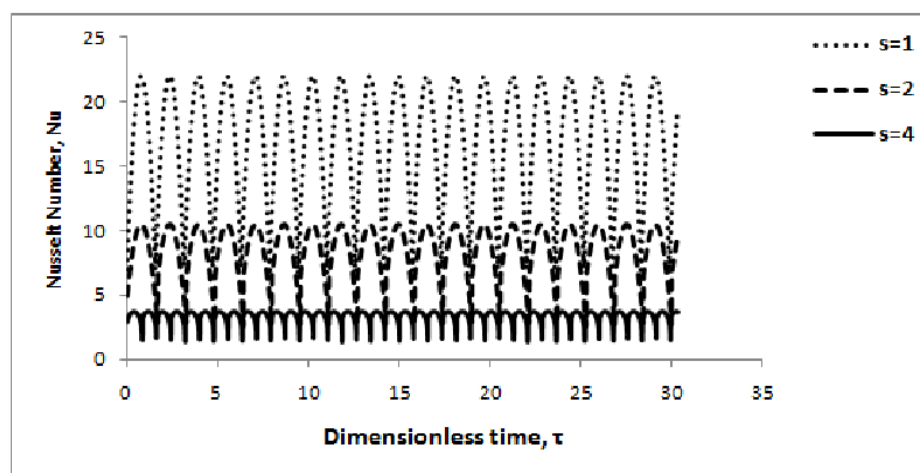


Fig. (14) The effects of oscillation frequency, S , on the Average Nusselt number at $Ri=1$

5. Conclusions

Numerical solutions for unsteady laminar mixed convection flow and heat transfer in a two-dimensional square enclosure have been presented. The enclosure is configured such that the bottom wall was at higher temperature than its top wall, while the two vertical walls were insulated. In addition, the top wall was moving horizontally by a certain sinusoidal motion. The natural convective flow is sustained due to the temperature gradients generated inside the enclosure while the forced convective flow is attained due to the movement of the sliding wall. Air was the working fluid with a constant Prandtl number of (0.7). The effects of the Richardson number variation, Aspect ratio and oscillation frequency on the streamlines, isotherms, and heat transfer characteristics are investigated. The results of this study shows that, when the period time was more than $(0 P_d)$ up to $(1/2 P_d)$, the velocity of the top lid is in the positive direction, and thus applies positive shear stress to the fluid layers. On the other hand, when the period time more than $(1/2 P_d)$ up to $(1 P_d)$, velocity of the top lid is in the negative direction, so it applies negative shear stress to the fluid layers. It is also shown that at $Ri = 0.01$, velocity profiles at (period time= $1/4 P_d$) and (period time= $3/4 P_d$) are mirror

symmetric. Similarly, this behavior happens at (period time= $1/2 P_d$) and (period time= $1 P_d$). However, at $Ri = 1, 100$ the symmetry of velocity profile decreases. It is also observed that the average Nusselt number increased when the Richardson number is decreased and the periodic steady state condition is reached more quickly at higher Richardson numbers. while an increase in the aspect ratio suppresses the heat flux on the heated wall. Furthermore, the results shows that, as the oscillation frequency of the sliding top wall decreases, the oscillation amplitude of average Nusselt number will increases at constant Richardson number.

REFERENCES

1. Oztop H.F., Dagtekin I., "Mixed convection in two sided lid driven differentially heated square cavity", *Int. J. of Heat and Mass Transfer*, 47 (2004) 1761-1769.
2. Sharif M.A.R., "Laminar mixed convection in shallow inclined driven cavities with hot moving lid on top and cooled from bottom" , *Applied Thermal Engineering* 27 (2007) 1036 1042.
3. Aydin O., "Aiding and opposing mechanisms of mixed convection in a shear and buoyancy-driven cavity" , *Int. Commun. Heat Mass Transfer* 26 (7) (1999) 1019–1028.
4. Guanghong Guo, Muhammad A.R. Sharif, "Mixed convection in rectangular cavities at various aspect ratios with moving isothermal sidewalls and constant flux heat source on the bottom wall" , *Int. J. of Heat and Mass Transfer*, 43 (2004) 465–475.
5. Mustafa Mahmud, "Mixed convection inside nanofluid filled rectangular enclosures with moving bottom wall" , *thermal science*, years 2011, Vol. 15, No. 3, pp. 889-903.
6. R. Iwatsu, J.M. Hyun, K. Kuwahara, "Mixed convection in a driven cavity with a stable vertical temperature gradient", *Int. J. Heat Mass Transfer* 36 (6) (1993) 1601–1608.
7. O. Aydin, W.J. Yang, "Mixed convection in cavities with a locally heated lower wall and moving sidewalls", *Numerical Heat Transfer A* 37 (2000) 695–710.
8. K.M. Khanafer, A.M. Al-Amiri, I. Pop, "Numerical simulation of unsteady mixed convection in a driven cavity, using an externally excited sliding lid" , *Eur. J. Mech. B Fluids* 26 (2007) 669–687.
9. M.M. Abdelkhalek, "Mixed convection in a square cavity by a perturbation technique", *Comput. Mater. Sci.* 42 (2008) 212–219.
10. Latif M. Jiji, "Heat Convection" Springer-Verlag Berlin Heidelberg, (2006).